# Preliminary Computational Study for Future Tests in the NASA Ames 9' x 7' Wind Tunnel

Jason M. Pearl*
*University of Vermont, Burlington, VT 05401, USA*

Melissa B. Carter†, Alaa A. Elmiligui‡, and Courtney S. Winski§
*NASA Langley Research Center, Hampton, VA 23681, USA*

Sudheer N. Nayani¶
*Analytical Services & Materials, Inc., Hampton VA 23666, USA*

**The NASA Advanced Air Vehicles Program, Commercial Supersonics Technology Project seeks to advance tools and techniques to make over-land supersonic flight feasible. In this study, preliminary computational results are presented for future tests in the NASA Ames 9' x 7' supersonic wind tunnel to be conducted in early 2016. Shock-plume interactions and their effect on pressure signature are examined for six model geometries. Near-field pressure signatures are assessed using the CFD code USM3D to model the proposed test geometries in free-air. Additionally, results obtained using the commercial grid generation software Pointwise® are compared to results using VGRID, the NASA Langley Research Center in-house mesh generation program.**

## Nomenclature

| | | |
|---|---|---|
| NPR | = | nozzle pressure ratio |
| Re | = | Reynolds number |
| M | = | Mach number |
| x | = | distance in the stream-wise direction, inches |
| y | = | distance in the vertical direction, inches |
| z | = | distance in the spanwise (lateral) direction, inches |
| $T_0$ | = | total Temperature, °R |
| $T_\infty$ | = | freestream static temperature, °R |
| $p_0$ | = | total pressure, psf |
| p | = | static pressure, psf |
| $p_\infty$ | = | freestream static pressure, psf |
| dp/p | = | non-dimensional over-pressure |

*Graduate Student, College of Engineering and Mathematical Sciences, AIAA Student Member.
†Aerospace Engineer, Configuration Aerodynamics Branch, Mail Stop 499, AIAA Senior Member.
‡Research Engineer, Configuration Aerodynamics Branch, Mail Stop 499, AIAA Senior Member.
§Aerospace Engineer, Configuration Aerodynamics Branch, Mail Stop 499, AIAA Senior Member.
¶Senior Scientist, CFD Group, 107 Research Drive, AIAA Senior Member.

# I. Introduction

The NASA Advanced Air Vehicles Program, Commercial Supersonics Technology Project seeks to advance tools and techniques to make over-land supersonic flights feasible. One of the major challenges presented by supersonic flight is increased aircraft noise. At supersonic speeds, shock and expansion waves form along the aircraft generating strong pressure waves (i.e., boom signatures), which can cause discomfort for people on the ground. As a result, commercial supersonic air travel has been restricted or banned in many countries. In light of this challenge, the evaluation and prediction of boom signatures using Computational Fluid Dynamics (CFD) is a high priority. A number of CFD codes have been examined and compared for this application at the NASA Boom Workshop of 2008[1] and the AIAA Boom Workshop of 2014.[2] As the High Speed Project has evolved the work has become more focused, examining different aspects of supersonic aircrafts and their relation to boom signature.

Recently, the effects of engine plume on the boom signature have been of particular interest. At the NASA Langley Research Center, the in-house CFD suite Tetrahedral Unstructured Software System (TetrUSS) has been employed to examine the plume effects on boom signature. The capabilities of the CFD code, USM3D, to accurately model supersonic jet plumes has been examined using benchmark nozzle flow cases.[3] Other studies have examined and identified meshing techniques best suited for capturing the propagation of the boom signature through the near- to mid-field regions.[4,5]

The present study builds upon these results, employing previously examined models and techniques to provide preliminary analysis for future experiments in the NASA Ames 9' x 7' Supersonic Wind Tunnel. Shock-plume interactions and the corresponding effects on boom signature are assessed for six different model geometries. Each model geometry is simulated in free-air conditions that match test conditions. Additionally, results using two meshing programs are compared: (1) VGRID part of the TetrUSS CFD suite and (2) Pointwise® a commercial grid generation software. The pressure signature, assessed at different distances below the model (7, 15, 25, and 35 inches), is used as a metric to compare different geometries and meshing methodologies. The models examined range in length from 22.3 to 25.0 inches, and as such, the region of interest (7-35 inches) for pressure signature analysis ranges from 0.3 to 1.5 body lengths below the model. See Figure 1 for an illustration of the pressure signature assessed at different distances.

# II. Experimental Test Information

The computational study presented in this paper is a preliminary examination of geometries slated for wind tunnel testing at the NASA Ames 9' x 7' Supersonic Wind Tunnel. The test section has a width of 9 feet and a height of 7 feet. A 7-foot long and 14-inch tall pressure rail will be fixed to the centerline of the tunnel sidewall to record boom signature measurements. The NASA Ames 9' x 7' Supersonic Wind Tunnel is a closed circuit, continuous flow wind tunnel that can operate between Mach 1.55 and Mach 2.55. For the proposed experiment, the tunnel will be run at a total pressure of 16 psi and a total temperature of 100°F.

## A. Geometries

The model geometry consists of three basic components: the cone-cylinder body containing the Putnam nozzle, the strut that anchors the model during wind tunnel testing, and a shock generator affixed to the strut or a deck attached to the bottom of the nozzle. Six different configurations are examined consisting of four shock generators and two decks. The four shock generators are designed to represent aircraft tail shocks and consist of: (1) a biconvex geometry at zero angle of attack (Figure 2), (2) a biconvex geometry at 4° angle of attack, (3) a double-wedge geometry (Figure 3), and (4) the 25D geometry (Figure 4). Two decks are examined, one backward-swept and the other forward-swept. These are shown in Figures 5 and 6, respectively.

Depending upon the configuration examined, the cylindrical body of the nozzle is elongated or shortened, to control the location of the plume internal shock structure. The models range in length from 22.3 to 25.0 inches. The Putnam nozzle used in this study has an expander half angle of 6.04° and an expansion area ratio of 1.722 yielding an optimal expansion NPR of 8.12. The internal nozzle geometry and the strut geometry are kept constant through all the tests.

# III. Numerical Techniques

## A. Computational Model

The CFD code USM3D is used for all computations. USM3D is a cell-center, finite-volume, Navier-Stokes flow solver for unstructured grids that is maintained by the NASA Langley Research Center. Several inviscid flux schemes, turbulence models, and limiters are available, selections of which are based on established best practices of applying USM3D to supersonic jet flows.[3,6]

Roe's flux differencing scheme (FDS) is employed to compute inviscid flux quantities.[7] The k-$\epsilon$ turbulence model with Sarker compressibility correction is used and has been shown to provide good results for supersonic jet flows.[8] A min-mod limiter is used to ensure numerical stability.

## B. Boundary Conditions

Boundary conditions are selected based on flow conditions in the test section of the Ames 9' x 7' Supersonic Wind Tunnel. At the freestream inlet, $M = 1.6$, $Re = 378,600/inch$, and $T_\infty = 370$ °R are specified. The freestream outlet boundary conditions are determined by extrapolating the internal flow field. At the inlet of the Putnam nozzle, the total temperature ratio ($T_0/T_\infty$), the total pressure ratio ($p_0/p_\infty$), and the normalized static pressure ($p/p_\infty$) are specified. The total pressure ratio and normalized static pressure at the nozzle inlet are set to 5.7144 and 5, respectively, yieldings a nozzle pressure ratio of 8. For this study, the pressure is normalized such that $p_\infty = 0.7143$. The total temperature ratio at the nozzle inlet is set equal to 1.8 and held constant across all simulations.

# IV. Mesh Generation

Computational meshes are generated using the LaRC in-house meshing programs in the TetrUSS CFD suite and the commercial grid generation software Pointwise®. To obtain accurate results, it is important for the mesh to contain proper resolution in key locations (i.e., the nozzle lip, boundary layers, and plume shear layer) while maintaining a reasonable number of cells ($N < 100$ million) in the volume grid. In the following sections, we will discuss the two different mesh generation processes.

## A. VGRID Meshes

The TetrUSS suite contains a set of programs (GridTool, VGRID, PostGrid, and BoomGrid) that are used to generate unstructured $3D$ tetrahedral meshes. CAD geometries are pre-processed in GridTool establishing the boundary surfaces and conditions of the computational domain. The unstructured grid generation program, VGRID, is used to generate the volume mesh. The mesh generation process is based on the Advancing-Front method (AFM)[9] and Advancing-Layers method (ALM).[10] Both methods utilize a marching process to grow tetrahedral cells from triangular surface meshes. Cell shape and size are controlled locally by user-defined sources. Careful placement of sources in VGRID is required to properly resolve flow features and obtain an accurate solution. Past works have established a sourcing scheme that provides appropriate resolution of the plumes shock structure and shear layer.[3,6] A set of 5 cylindrical and conical volume sources are used to control cell density in the internal plume region. Line sources are then used to further refine the nozzle lip and other features of the model geometry. This sourcing methodology is utilized in the present study for meshes constructed using VGRID. After creation of the volume mesh in VGRID a set of post-processing programs are utilized to create the final mesh. PostGrid is used to improve cell quality and close open pockets within the mesh. The final step in the meshing process utilizes BoomGrid to shear and stretch the outer mesh region to align with the free-stream Mach angle. This prevents numerical dissipation caused by excessive refinement, allowing the pressure signature to propagate several body lengths below the model. This process has been used successfully in the past to study the pressure signature of model geometries.[11]

## B. Pointwise® Meshes

In Pointwise®, cell shape and size in a volume (or block) is controlled by its boundary surfaces, and likewise, the distributions of cells on the surfaces are controlled by their boundary curves. A volume mesh block requires at a minimum a fully closed set of surface meshes; however, additional surfaces, internal to

the domain (baffle surfaces) can also be defined to further control mesh structure. Unstructured triangular surface meshes can be constructed using AFM or the Delaunay triangulation algorithm. Volume meshes are then created using an anisotropic tetrahedral extrusion method via the T-Rex® feature for boundary layers and a Modified Delaunay algorithm for the remainder of the volume.

In this study, Pointwise® meshes are created to imitate the best practice sourcing methodology established for VGRID. This is accomplished by dividing the domain into two distinct mesh blocks: (1) a quasi-cylindrical block of highly resolved cells that hugs the model geometry and (2) an extended conical region of high aspect ratio cells stretched along the free-stream Mach angle, which encircles the quasi-cylindrical block. An illustration of the two mesh blocks is provided in Figure 7. On the left of Figure 7, a view of the internal quasi-cylindrical block is outlined in magenta. On the right of Figure 7, a view of the external stretch block is shown with the edges of the bounding surfaces and baffle surface shown as magenta lines. The edge of the internal mesh block can also be seen as a magenta rectangle that surrounds the model and plume baffle surface.

Within the internal quasi-cylindrical block, line sources are used to properly resolve key feature of the model (i.e., the nozzle lip, leading and trailing edges) and baffle surfaces are used to control cell density and shape in the plume. The plume source consists of a cylindrical baffle surface extending from nozzle lip downstream and is pictured in Figures 8 and 9(b). The cylindrical baffle, is comprised of two sections: (1) a truncated cone near the nozzle exit used to resolve the growth of the plume shear layer and (2) a constant radius cylinder extending downstream for the remainder of the plume. The T-Rex® feature is used to resolve the boundary layer on the model and the remainder of the tetrahedral volume mesh is created using the Modified Delaunay algorithm.

The external stretch-region block is bound by two cones extending 5+ body lengths radially from the model. Within the stretch region a set of 20-30 parallel conical baffle faces are used to control the cell orientation and size in the block. An image showing the outline of the external block and the baffle surfaces it contains is shown in Figure 7(b). The majority of the volume mesh in this region is created using the T-Rex® feature. The baffle faces are used as artificial walls during the mesh generation process and cells are grown from the baffle faces with the layer thickness held constant. This yields a mesh with constant cell density in the direction perpendicular to the Mach angle and a parallel stretching defined by the distribution on the baffle surface. It is important that the baffle surface distribution does not cause any sharp changes in cell size and shape (i.e., smooth variations in cell type are desired). As such, the baffle surfaces are highly refined near their interface with the internal quasi-cylindrical block, providing a nearly isotropic mesh with cell density equivalent to the internal mesh block. Further from the internal mesh block, the baffles contain larger surface cells. This causes the corresponding adjacent volume cells in the T-Rex® generated layers to be high aspect ratio cells, stretched along the Mach angle. A plot of the cell aspect ratio (stretching) is provided in Figure 10. Here the isotropic cells near the internal mesh block are shown in green. High aspect ratio cells farther from the internal mesh block are shown in red.

## V. Results

Four different shock generators, designed to represent an aircraft tail shock, are examined and two different deck geometries are compared using VGRID to generate computational meshes. Results from the VGRID mesh are then compared to a Pointwise® mesh for the biconvex geometry.

### A. Shock Generator Geometries

Pressure signatures extracted from 7 inches below the nozzle center-line are plotted in Figure 11(a) for the four shock generator geometries. Features of the pressure signatures that remain constant for all 4 configurations are labeled. The *Nose Shock* originates from the tip of the nose cone. The *Cone-Cylinder Expansion* is an expansion wave that originates from the point in the geometry at which the forward nose cone blends into the cylinder of the body. The strut shock originates from where the strut connects to the nozzle body. The *Aft-Nozzle Expansion* originates from the tapering of the body cylinder near the nozzle lip, and finally, the *Nozzle Lip Shock* originates from the nozzle lip and is caused by the free stream flow turning around the exhaust plume.

The portion of the pressure signature affected by changes in shock generator geometry is magnified and shown in Figure 11(b). Here the leading edge (LE) and trailing edge (TE) shocks of each of the shock

generators are labeled. The 25D LE shock is masked by the *Aft-Nozzle Expansion*. The 25D geometry exhibited the weakest over-pressure (dp/p=0.02) but a strong under-pressure (dp/p=-0.06). The biconvex geometries, had pressure signatures bound by |dp/p|=0.04. The 4° angle of attack biconvex geometry exhibited a stronger LE shock but a weaker expansion and TE shock when compared to the zero angle of attack biconvex geometry. The double wedge geometry exhibited the strongest over- and under-pressure of the geometries examined with a maximum dp/p of 0.1 and a minimum of -0.1.

### B. Deck Geometries

Pressure signatures (dp/p) extracted from 7 inches below the nozzle center-line are plotted in Figure 12(a) for the two deck geometries. Again the *Nose Shock* and *Cone-Cylinder Expansion* are labeled. The shock originating from the front of the deck is also identified. A zoomed view of the region of the pressure signature that varies between the two deck geometries is shown in 12(b). The backward-swept deck has a maximum under-pressure of approximately dp/p=-0.015, originating from the tapering of the deck near the aft end. The forward-swept deck exhibited a stronger under-pressure from this location with dp/p=-0.04.

### C. Comparison of Meshing Programs

The biconvex geometry is used as a test case to compare meshes created using VGRID and Pointwise®. Pressure signatures are compared in Figure 13 for the two meshing programs. The pressure signatures 7 inches and 35 inches below the nozzle centerline are shown in figures 13a and 13b, respectively. The stream-wise locations of peaks and troughs in the pressure signatures agree well between the two meshes. The Pointwise® mesh predicts under- and over-pressures of a slightly smaller magnitude. The relative magnitude of the disparity between the two meshes does not seem to change between the 7 inch and 35 inch cuts. This suggests that the discrepancy in results is likely caused by differences in the mesh density in the region near the model surface. The Pointwise® mesh appears to have a similar reduction in dp/p magnitude with distance across the stretch region as the VGRID mesh.

## VI. Conclusions

In this study, we present preliminary CFD results, analyzing six different model geometries that will be the subject of a wind tunnel test in the NASA Ames 9' x 7' Supersonic Wind Tunnel early next year. Results from this test will be used as part of a validation exercise examining the ability of the USM3D code and the current meshing techniques to accurately predict shock plume interactions. As such, a wide variety of geometries providing a wide variety of pressure signatures have been examined. Four shock generators designed to represent the shock from an aircraft tail were simulated. Of the four, the double wedge provides the largest over and under-pressures. Additionally, the 25D configuration exhibited a strong under-pressure but modest over-pressures due to shock cancellation. The smaller biconvex geometries had the smallest variations in pressure signature. Of the two deck geometries, the forward-swept deck provided the largest under- and over-pressures.

As part of this study, the capabilities of the Pointwise® grid generation software (in comparison to VGRID) for the application of supersonic pressure signature analysis were examined. The Pointwise® mesh slightly underpredicted the magnitude of the under- and over-pressures from the VGRID mesh; however, the level of underprediction was consistent at all distances below the model (i.e 7, 15, 25, and 35 inches). This suggests that the Pointwise® mesh did not introduce unacceptable error or numerical diffusion within the stretch region and that the discrepancy likely arose from differences in cell density in the non-stretch near field. Further testing is required to develop a best practice meshing methodology for applying Pointwise® to this particular application.

## VII. Acknowledgements

The research reported in this paper was sponsored by the NASA Advanced Air Vehicles Program Commercial Supersonics Technology Project and the University Space Research Association (USRA).

# References


[1]Park, M. A., Aftosmis, M. J., Campbell, R. L., Carter, M. B., Cliff, S. E., and Bangert, L. S., "Summary of the 2008 NASA Fundamental Aeronautics Program Sonic Boom Prediction Workshop," *Journal of Aircraft*, Vol. 51, No. 3, August 2014, pp. 987–1001.

[2]"1st AIAA Sonic Boom Prediction Workshop," *1st AIAA Sonic Boom Prediction Workshop*, AIAA, n.d. Web. 06 June 2015 <http://lbpw.larc.nasa.gov/>.

[3]Carter, M. B., Nayani, S., Elmiligui, A. A., and Campbell, R. L., "USM3D predictions of Supersonic Nozzle Flow," AIAA-2014-2270, June 2014.

[4]Campbell, R., Carter, M., Deere, K., and Waithe, K., "Efficient Unstructured Grid Adaptation Methods for Sonic Boom Prediction," AIAA-2008-7327, August 2008.

[5]Carter, M. and Deere, K., "Grid Sourcing and Adaptation Study Using Unstructured Grids for Supersonic Boom Prediction," AIAA-2008-6595, August 2005.

[6]Carter, M. B., Elmiligui, A. A., Nayani, S., Castner, R. S., Bruce, W. E., and Inskeep, J., "Computational and Experimental Study of Supersonic Nozzle Flow and Shock Interactions," AIAA 2015-1044, January 2015.

[7]Roe, P., "Characteristic Based Schemes for the Euler Equations," *Annual Review of Fluid Mechanics*, Vol. 18, 1986, pp. 337–365.

[8]Pandya, M., Abdol-Hamid, K., and Frink, N., "Enhancement of USM3D Unstructured Flow Solver for High-Speed High-Temperature Shear Flows," AIAA-2009-1329, January 2009.

[9]Lohner, R. and Parikh, P., "Three-Dimensional Grid Generation by teh Advancing Front Method," *Iinternational Journal of Numerical Methods in Fluids*, Vol. 8, 1988, pp. 1135–1149.

[10]Pirzadeh, S., "Three-dimensional unstructured grids by the advancing layers method," *AIAA Journal*, Vol. 34, No. 1, January 1996, pp. 43–49.

[11]Carter, M., Campbell, R., and Nayani, S., "USM3D Analysis of Low Boom Configuration," AIAA-2011-3335, August 2011.

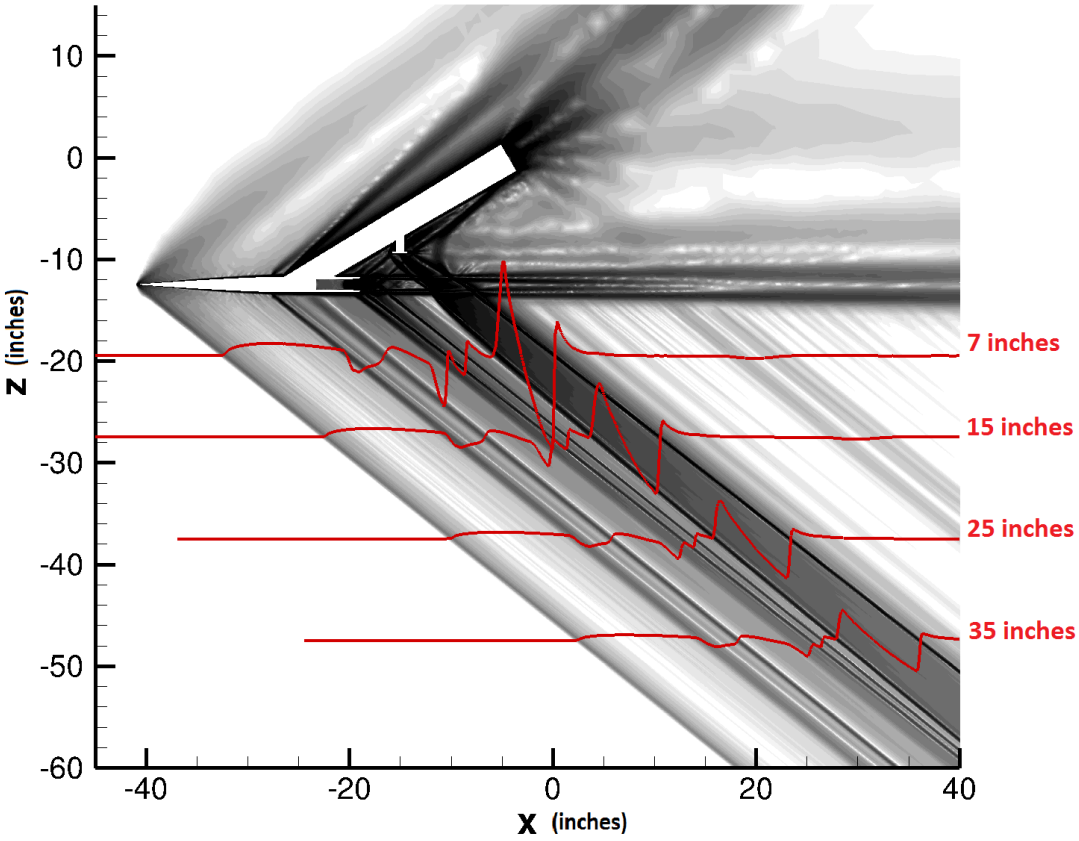


**Figure 1. Schlieren image of the double wedge geometry produced from VGRID mesh with pressure signatures at different distances overlain in red. Pressure signatures are displayed for 7, 15, 25, and 35 inches below the model centerline.**

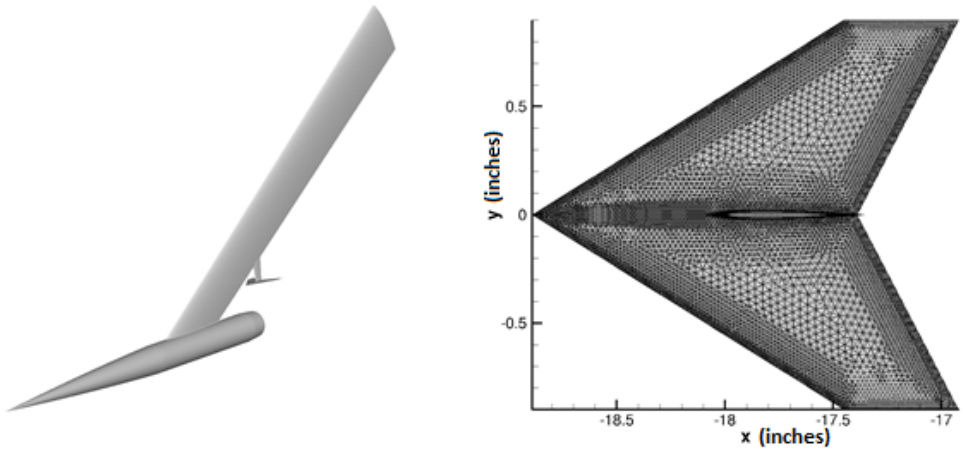


**Figure 2. Isometric view (left) of the model geometry with a top view (right) of the biconvex shock generator with VGRID mesh surface.**

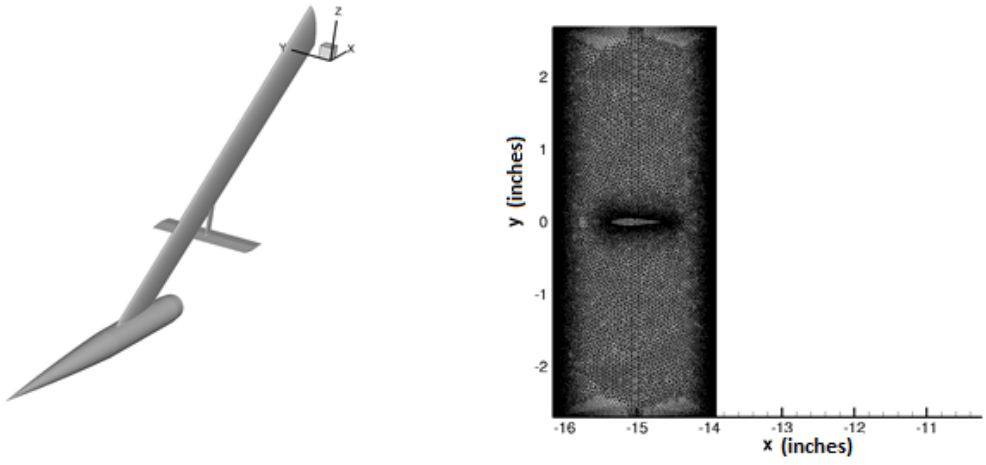


**Figure 3. Isometric view (left) of the model geometry with a top view (right) of the double wedge shock generator with VGRID mesh surface.**

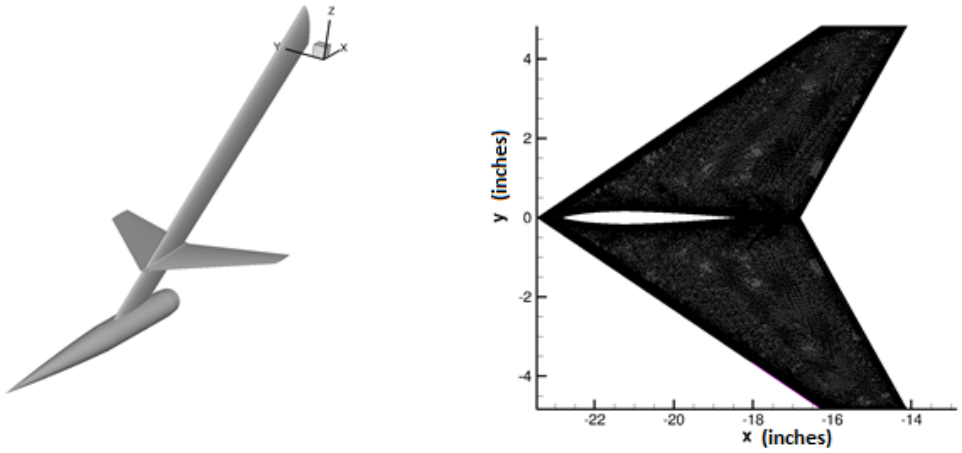


**Figure 4. Isometric view (left) of the model geometry with a top view (right) of the 25D shock generator with VGRID mesh surface.**

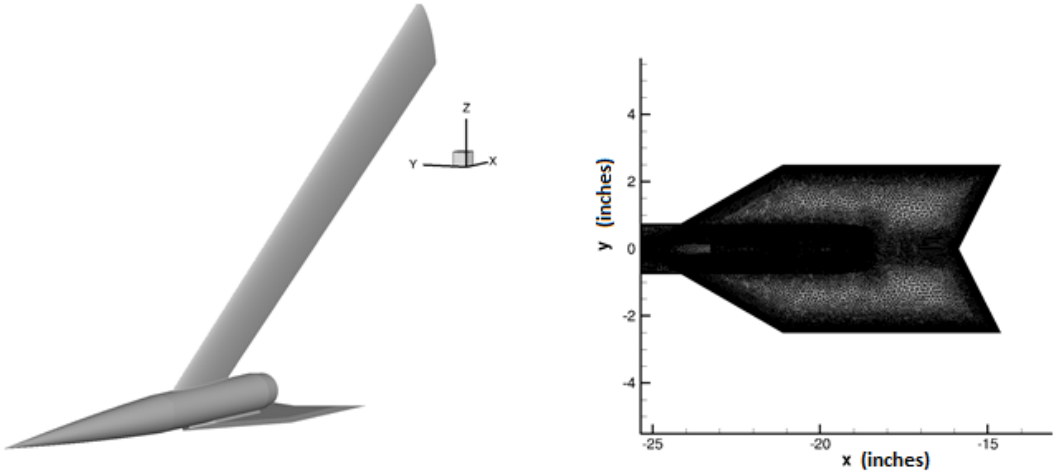


**Figure 5. Isometric view (left) of the model geometry with a top view (right) of the backward-swept deck with VGRID mesh surface.**

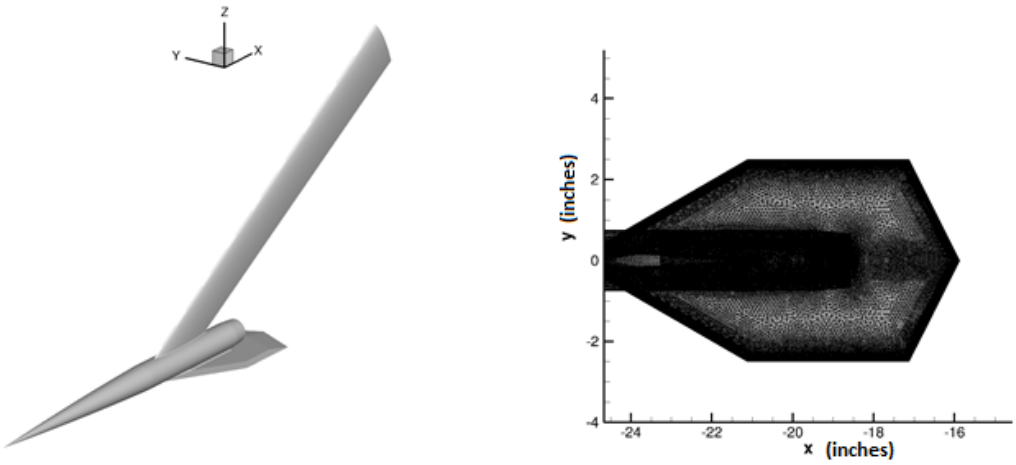


**Figure 6. Isometric view (left) of the model geometry with a top view (right) of the forward-swept deck with VGRID mesh surface.**

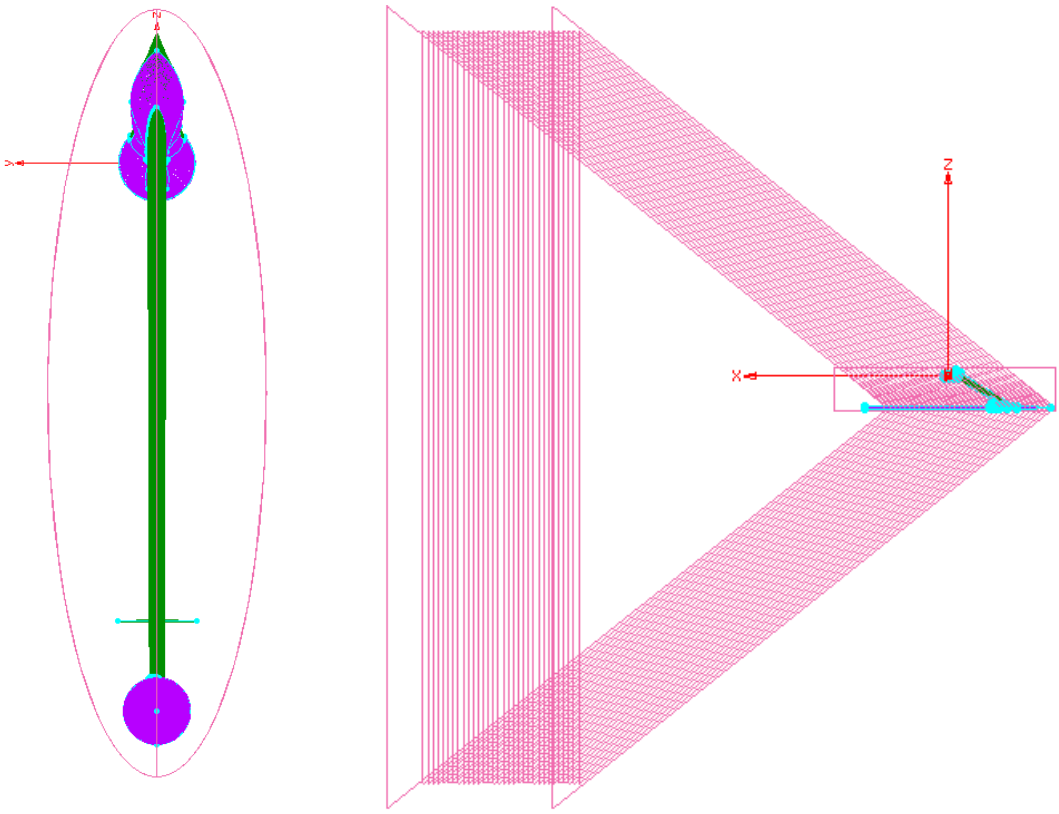


(a) Edge of internal block

(b) Edges of external block and its constituent baffle faces

**Figure 7. Illustration of the block structure employed to create the Pointwise® volume mesh. (Left) View of the internal quasi-cylindrical block which hugs the model surface. (Right) View of the external block and baffle surface edges.**

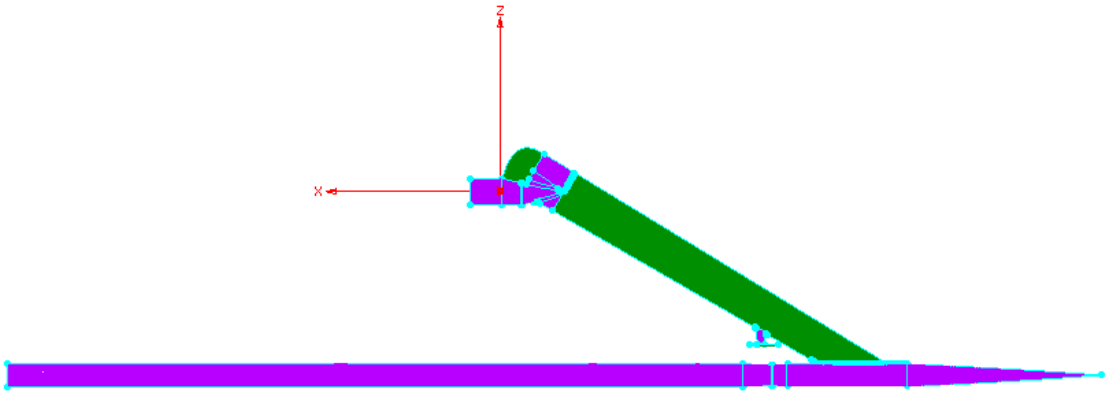


**Figure 8. Side view (from y+ axis) of Pointwise® model surface mesh and plume baffle surface.**

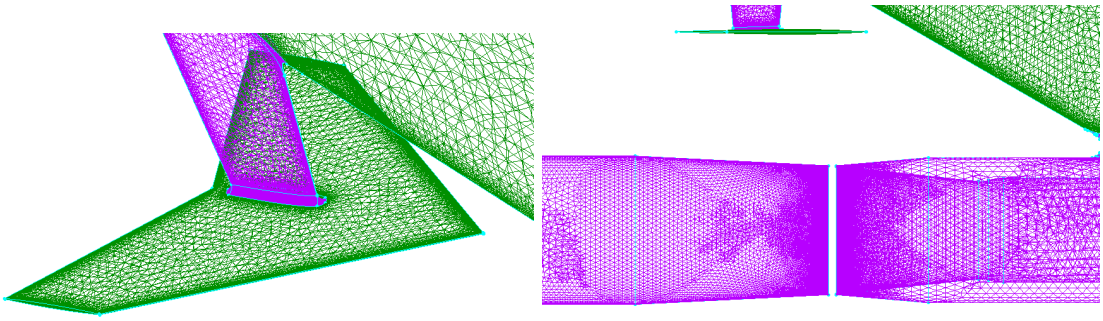

(a) Shock generator (b) Nozzle lip

**Figure 9. Zoomed views of the Pointwise® surface mesh. (Left) View of the mesh refinement on the leading and trailing edge of the shock generator. (Right) View of the mesh refinement near the nozzle lip.**

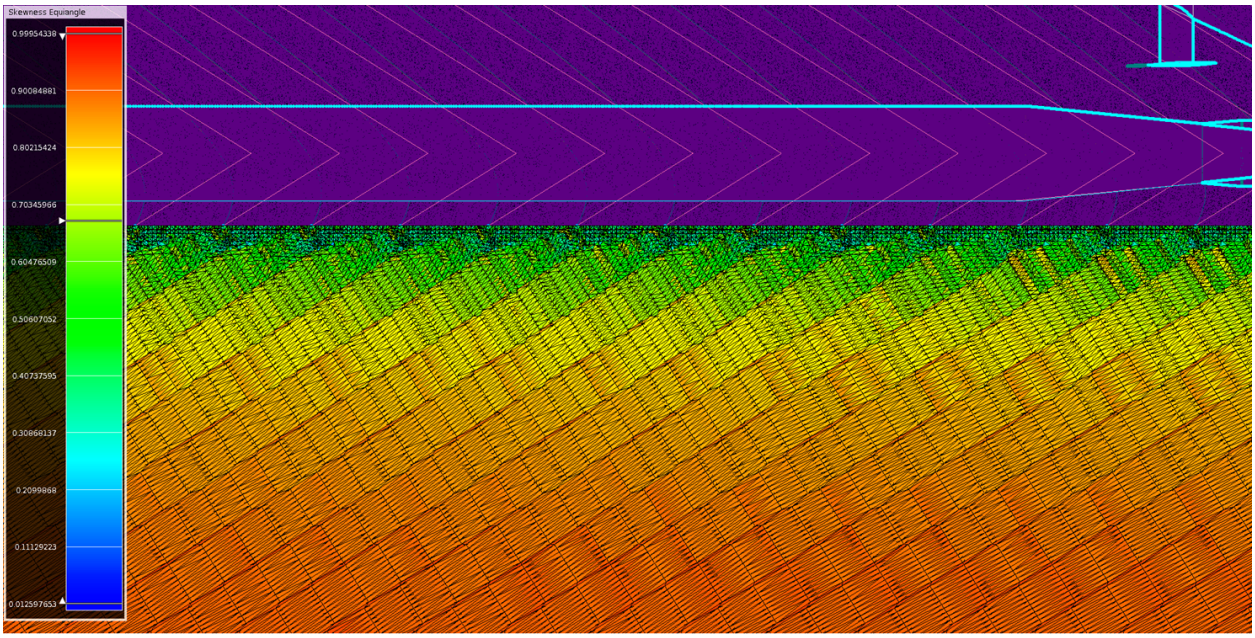


**Figure 10. Cells in the external stretch region block created using Pointwise's® T-Rex® feature to grow cells from parallel baffle faces. Cells are color coded by aspect ratio. Green indicates approximately isotropic cells and red indicates high aspect ratio stretched cells.**

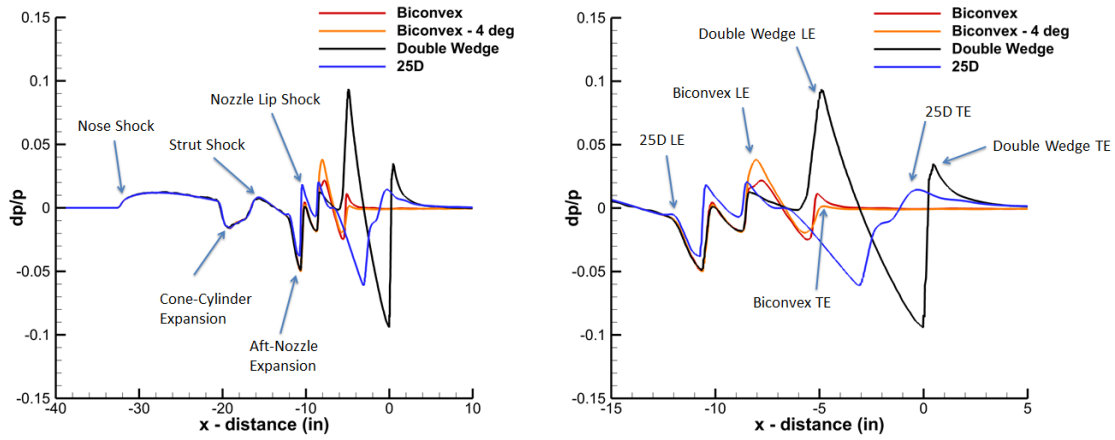


(a) Full signature

(b) Zoomed region of interest with leading edge and trailing edge shocks labeled.

**Figure 11. Pressure signatures at 7 inches below the model are shown for the four shock generators examined using VGRID meshes.**

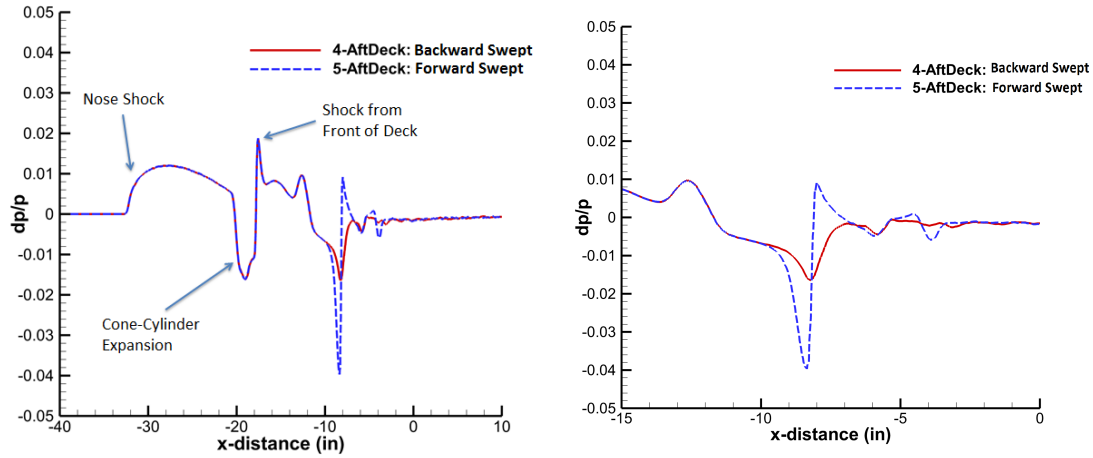


(a) Full signature

(b) Zoomed region of interest

**Figure 12. Pressure signatures at 7 inches below the model are shown for the two aft deck geometries examined using VGRID meshes.**

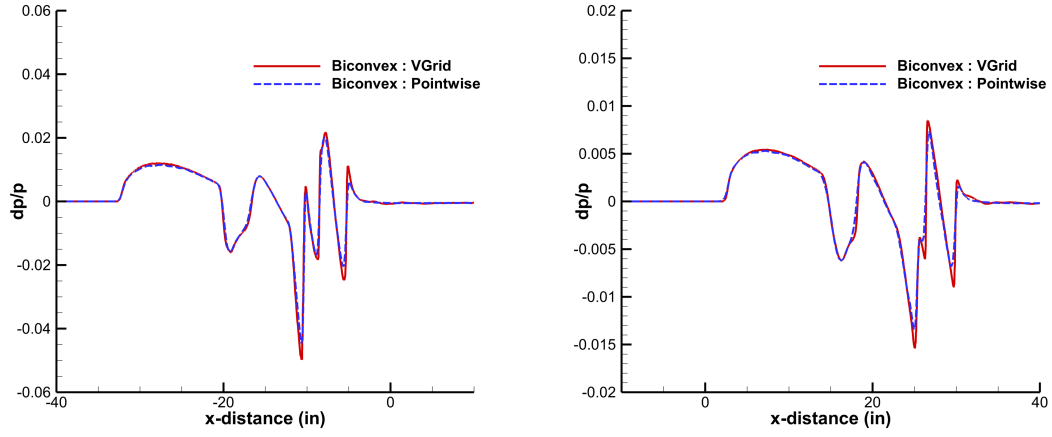


(a) 7 inches

(b) 35 inches

**Figure 13. Comparison of the pressure signature for the biconvex geometry between the Pointwise® and VGRID meshes at 7 inches and 35 inches below the model.**